Dopant (Mn, Fe, Co and Cu) effects on the structure and dielectric dispersion mechanisms in relaxor PLZT ceramics

Dopant (Mn, Fe, Co and Cu) effects on the structure and dielectric dispersion mechanisms in relaxor PLZT ceramics

V I Dimza

Institute of Solid State Physics, University of Latvia, LV-1063 Riga, Latvia

Abstract. The PLZT 8/65/35 compound, commonly known for relaxor behaviour, as well as PLZT 8/65/35+Me compositions (Me $\equiv$ 3d elements (Mn, Fe, Co or Cu)) is examined, a number of different techniques being used:

(1) dielectric measurements of complex permittivity $\varepsilon(\nu, T, E)$ at frequencies from 10^{-1} to 10^7 Hz in the range of temperatures from 0 to 200 °C;

(2) Raman scattering (RS), EPR and x-ray diffraction.

The behaviour of $\varepsilon(\nu, T, E)$ is interpreted assuming the existence of three different polarization mechanisms, the partial contributions to the dielectric constant of which depend on the dopant concentration and the ranges of frequencies, temperatures or field intensities. Structural criteria are proposed to evaluate the contributions from each of the mechanisms.

1. Introduction

The microscopic origin of a diffuse phase transition is one of the current problems of ferroelectrics (FE) [1]. Because of specific phenomena observed in complicated ABO_3 compositions with a broad $\varepsilon(T)$ (dielectric permittivity temperature dependence) maximum, e.g. (lead lanthanum zirconate–titanate (Pb, La) (Ti, Zr)O_3 8/65/35 (PLZT 8/65/35) where 65/35 is the atomic percentage ratio of zirconium to titanium, and 8 is the atomic percentage of La substituted for Pb) and a number of Pb(B′B″)O_3 compounds, e.g. (PbMg$_{1/3}$Nb$_{2/3}$O$_3$) (PMN) [4, 5], these materials are related to the class of relaxor FE [2–7]. The macroscopic spontaneously polarized state does not appear and a cubic structure is detected by x-ray diffraction (XRD) at temperatures as low as liquid-nitrogen temperature (at the same time the temperatures $T_{m\varepsilon}$ of the $\varepsilon(T)$ maximum for PLZT 8/65/35 and PMN materials at 1 kHz are about 90 °C and 0 °C, respectively). On the other hand, a pronounced relaxation (i.e. relaxor behaviour) is demonstrated over a wide interval (about 200 °C) of temperatures around $T_{m\varepsilon}$ by dielectric [8, 9], elastic [10, 11], electromechanical and electro-optic [12] parameters. Analysis of the relaxation time τ dependence on temperature [5–7] has shown that the distribution of τ strongly broadens, extending to macroscopic time intervals at some freezing temperature T_f ($T_f < T_p < T_{m\varepsilon}$; T_p is the temperature of remnant polarization breakdown) [5, 7] which is referred to as 'glass-like' behaviour. There are a number of arguments [5, 10–18] supporting the appearance and involvement in the processes of polar nanoregions (about 50 Å). In the first approximation the polar nanoregions appearing at 330–340 °C [10, 11, 13, 14] may be considered to be relaxing and fluctuating at $T > T_f$, but frozen and static at $T < T_f$ [5, 7].

However, at present more questions than answers are to be found in the reports available on experimental studies of relaxor behaviour. The first attempt to expound relaxor behaviour

was made by Isupov [2] and Smolensky [3], and later by Bokov [4] and Cross and co-workers [5–7]. According to this version, relaxor materials consist of small (about 50–100 Å) nanoregions each of which, because of a different composition, has its own different individual local phase transition temperature T_{cloc} and local but ordinary FE behaviour. In PLZT [19], T_{cloc} is supposed to be higher in regions rich in Pb and Ti while lower in regions rich in La^{3+}, Zr and vacancies (V_A) in the Pb lattice [14]. Now this model is assumed to be at least oversimplified, if not wrong [5–11, 15, 18]. More recent models accepting compositional disorder as a necessary condition do not accept the possibility of local phase transitions proposed by Smolensky and Isupov. On the other hand, it is quite obvious that only compositional fluctuations cannot explain relaxor behaviour. Really, the studies of some $Pb(B'B'')O_3$ structures such as PMN suggest that the coexistence of compositionally ordered ($[Mg]/[Nb] = 1/1$) and disordered (Nb-rich) nanoregions is important [4, 15, 16]. Regarding compositional conditions for the appearance of polar nanoregions [2, 9, 16], PLZT 8/65/35 [19] seems to be completely different from PMN or PSN [5, 17, 18]. There is no reason to expect ordered Ti and Zr 1/1 regions (equal charge and little difference in ion masses). There is a sharp transition in PZT (compositionally disordered material [20]), and relaxor properties appear at certain concentrations of La introduced into PZT (depending on the [Ti]/[Zr] ratio). The role of La^{3+} in relaxor behaviour is not clear. Do La^{3+} ions disturb translational symmetry as defects? Why do they shift the morphotropic phase boundary at the same time [2, 19]?

The real nature of polar nanoregions in PLZT is not clear since neither compositional and structural elements nor dynamics, interactions and circumstances of freezing are known [19]. Concerning the reasons responsible for the nearly monodispersive (probably Debye-type [22–24]) relaxation at $T > T_{m\varepsilon}$ [6–9], the question of elementary relaxing particles [15], i.e. the 'seeds' or 'nuclei' of polar nanoregions, is important [21]. A similar structural (but not compositional) pattern of elementary relaxing particles might be acceptable considering the 'crossover' problem (crossover from displacive to order–disorder behaviour in structural phase transitions upon approaching T_c) in $BaTiO_3$ (BT) [25–27]. A relaxing TiO_6^{2-} octahedron, obviously, plays there the role of an elementary relaxing particle; it is primarily regarded as a Ti ion jumping between equivalent off positions (i.e. Ti as an 'off-site ion') [26]. Such relaxation in BT contributes to the non-displacive component of dielectric permittivity [25] and causes symmetry breaking and the appearance of broad forbidden (because they appear at $T > T_c$, i.e. in the cubic phase) Raman bands [28], which are the source of dynamical structural disorder in the 'crossover' temperature region [25–27]. The order–disorder behaviour of the Raman scattering pattern of relaxor-type PLZT ceramics is similar [29–32]): firstly a broad central peak, which might compensate the seeming absence of the soft mode in relaxor structures [31] and secondly broad bands below 100 cm^{-1}, i.e. there is a 'glass-like' behaviour of spectra, the bands being 'forbidden', since cubic structure is observed by XRD. The appearance of the bands may be considered as a result of local dynamic disorder. Fitting with the Curie–Weiss law and a large value of Curie–Weiss constant C_{CW} at high frequencies (9 GHz) and temperatures (above 330 °C) provide at the same time evidence of pre-critical or soft-mode behaviour [33].

Also, a number of papers have appeared considering some other dielectric problems which are important, in our opinion, for understanding relaxor behaviour, too:

(a) the microscopic nature of the FE state in ABO_3 materials which is predominantly related to the high polarizability of oxygen, its anisotropy and non-linearity [34]; not only the size of A and B ions but also the structure of the electron shell of the ions is important (the Ti off-site ion problem in BT may also be considered with respect to this [34]);

(b) the problem of dipole glass in $(K, Li)TaO_3$ and $K(Ta, Nb)O_3$ [35–41];
(c) the universal many-body dielectric response model in disordered systems [22–24].

To obtain experimental data related to relaxor properties of PLZT electro-optic ceramics a number of different techniques have been used in the present study: dielectric spectroscopy to find the $\varepsilon^*(\nu, T, E)$ curves at frequencies from 10^{-1} to 10^7 Hz in the range of temperatures from 0 to 200 °C (ε^* is the complex dielectric constant, given by $\varepsilon^* = \varepsilon' - i\varepsilon''$), Raman scattering (RS), EPR and XRD (at 20 °C). Most essential conclusions are obtained from the analysis of $\varepsilon^*(\nu, T)$ and structural effect correlations on changing the composition, i.e. the [La]/[Pb] and [Ti]/[Zr] ratio, and at the doping relaxor composition PLZT 8/65/35 by Mn, Fe, Co and Cu.

2. Samples and methods

The PLZT 8/65/35 compound commonly known for relaxor behaviour as well as PLZT 8/65/35+Me compositions (Me $\equiv$ 3d elements (Mn, Fe, Co or Cu) (the total amounts [Me_{tot}] concentration of added Me atoms being 0.01; 0.1 and 1.0 wt.%) with modified properties were examined.

Samples were obtained by the two-stage hot-pressing techniques [42, 67]. Also to change the valency (degree of oxidation) of Me ions the samples were subjected to special treatment during production or after it. The EPR spectra of Fe in PLZT 8/65/35+1 wt.% Fe are shown in figure 1(d) for three different exposure times (0.5, 3.0 and 20 h) in the second stage of hot-pressing conditions: 1200 °C in PbO atmosphere at 200 kgt cm^{-2} uniaxial pressure. Since the first stage is performed at 970 °C in Al_2O_3 dies in an atmosphere at 10^{-4} Torr at 300 kgt cm^{-2} pressure for 30 min, oxidation, e.g. $Fe^{3+} \rightarrow Fe^{4+}$, proceeds with increase in the exposure time. It should be noted that the usual hot-pressing techniques used to obtain the rest of the doped and undoped PLZT 8/65/35 samples corresponded to the exposure time $t_e = 20$ h. It should also be noted [42, 45] that dopant effects are due to Me ions distributed in the B lattice denoted Me_l), i.e. they are not related to dopants distributed on grain boundaries, to dopant cluster formation, to change in grain size or to space-charge fields. Detailed descriptions of EPR [46, 67], dielectric measurements [43, 44], RS [30] and XRD [42] techniques have been reported elsewhere.

3. Experimental results and discussion

3.1. Dielectric permittivity dispersion (mechanisms of polarization in weak fields)

3.1.1. Undoped PLZT. To provide a better representation of polarization mechanisms for the PLZT 8/65/35 composition the $\varepsilon(\nu)$ curves presented (figure 2, curve 1) are combined from results of 10^{-1}–10^3 Hz [43, 44] and 10^4–10^7 Hz [42] measurements at $T = T_{m\varepsilon}+10$ °C. This temperature has been selected to show two frequency intervals, namely III and II, with different polarization mechanisms, i.e. a monotonous decrease in $\varepsilon''(\nu)$ and a maximum of $\varepsilon''(\nu)$ at ν_{IIm}, respectively. As the temperature is lowered, the regions of the two mechanisms become less pronounced; ε'' decreases monotonically in the whole frequency interval 10^{-1}–10^7 Hz and the two mechanisms merge so that they are difficult to distinguish.

At frequencies higher than 10^5 Hz a nearly monodispersive, i.e. Debye-like, relaxation (semicircle Cole–Cole diagrams $\varepsilon''(\varepsilon')$) is observed in undoped PLZT 8/65/35 samples (figure 2, curve 1, frequency interval II). Such behaviour has been reported [8, 9] in similar PLZT relaxor compositions lacking, however, the low-frequency interval below 10^2 Hz,
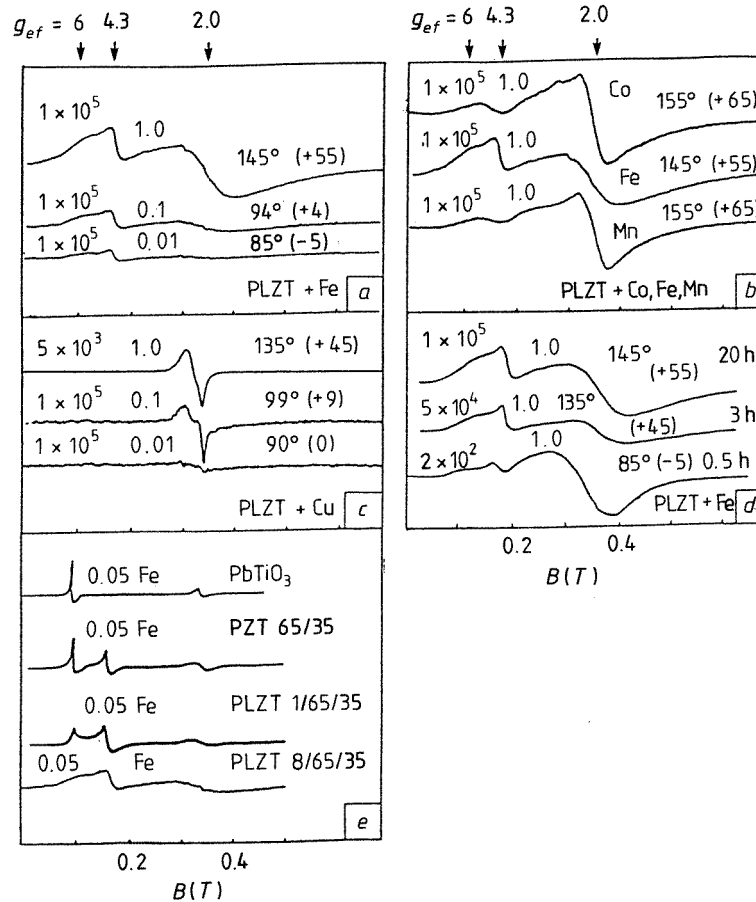
Figure 1. X-band absorption spectra of (b) Mn, (a), (b), (d), (e) Fe and (c) Cu in PLZT 8/65/35 ceramics at room temperature. The numbers on the curves (from left to right) for (a)–(d) are as follows: 1×10^5, 5×10^4, 5×10^3, 2×10^2, gain; 0.01, 0.1, 1.0, dopant concentration [Me_{tot}], in weight per cent; $85°$, $90° \ldots$, $145°$, temperature (in degrees Celsius) of the $\varepsilon(T)$ maximum $-T_{m\varepsilon}$ at 10^4 Hz; (-5), (0), $\ldots$, $(+55)$, $\Delta T_{m\varepsilon}$, the change in $T_{m\varepsilon}$ ($T_{m\varepsilon}$ of undoped PLZT 8/65/35 is usually $90\,°C$). The sample masses are the same in all cases (a)–(d) so that, assuming that the spectra of Mn, Fe and Co being due to d^5 ions (and Cu to d^9), the area S under absorption curve corrected for the gain is proportional to the concentration of d^5 (or Cu^{2+}) ions, i.e. $S_{d^5} \sim [Me_{ld^5}]$ (or $S_{d^9} \sim [Me_{ld^9}]$). 0.5 h, 3 h, 20 h in (d) denote the exposure to oxidizing environment during the second stage of hot pressing, the 0.5 h $\rightarrow$ 20 h corresponding to the $Fe^{3+} \rightarrow Fe^{4+}(Me_{ld^4} \rightarrow Me_{ld^5})$ process [67]. The first stage of hot pressing is at $970\,°C$ and 10^{-4} Torr, i.e. a reducing atmosphere. The 20 h exposure complies with the common PLZT 8/65/35 and PLZT+Me production technology, and to $[Me_{ld^4}] \gg [Me_{ld^5}]$, and the 0.5 h to exposure to $[Me_{ld^5}] > [Me_{ld^4}]$.

and Debye relaxation being the only mechanism discussed so far. Some workers [8] relate dispersion to polar microregions but object to any local phase transitions, as in the Isupov–Smolensky [2, 3] relaxor model. Other workers [9], considering the phase diagram in La, Pb/Ti/Zr coordinates at $20\,°C$ [2, 19], suggest that this relaxation is due to the tendency of O_6^{2-} octahedra to rotate in elementary cells containing Zr and La and to stretch in cells containing Ti and Pb, i.e. as a result of additional degrees of freedom due to compositional
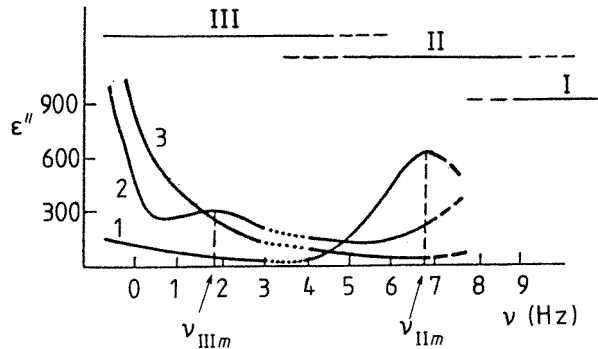
Figure 2. $\varepsilon''(\nu)$ at $T = T_{m\varepsilon} + 10\,^{\circ}$C; where $T_{m\varepsilon}$ is the temperature of the $\varepsilon(T)$ maximum at 10^4 Hz and $\varepsilon^* = \varepsilon' - i\varepsilon''$: curve 1, undoped PLZT 8/65/35; curve 2, 1 wt.% Fe doped (a similar curve is also observed for 1 wt.% Co); curve 3, 1 wt.% Mn doped; I, expected soft-mode frequency region; II, region of nearly Debye relaxation (switching of elementary relaxing particles) for undoped PLZT 8/65/35; III, region of elastic reversible phase boundary motion (curve 2) and irreversible phase boundary motion (curves 1 and 3); ν_{IIm} and ν_{IIIm}, the frequencies of $\varepsilon''(\nu)$ maxima, characteristics of elementary relaxing particle switching and elastic reversible phase boundary motion mechanisms, respectively.

disorder. It is essential to note that earlier work [8, 9] as well as the present analysis (figure 2) show the critical behaviour of ν_{IIm}, ε_l and ε'_h (ε'_l and ε'_h are the values of ε' at the low- and high-frequency ends, respectively, of the Cole–Cole diagrams where the semicircle intersects the ε' axis), which seems to demonstrate intrinsic instability.

To understand the nature of relaxation mechanism II (according to figure 2) it seems to be essential that the same kinds, i.e. Debye type, of relaxors are present in PZT ceramics [47, 48] before the PLZT solid solution is formed, the deepest dispersion and the maximum contribution to dielectric permittivity from that mechanism being observed at a Zr : [Zr]/[Ti] $\approx$ 50/50, i.e. at the morphotropic phase boundary between tetragonal and rhombohedral phases. Relaxors of similar properties are also found in BT [49] and seem to be manifestations of Ti as the off-site ion and 'crossover' behaviour [25–27]. In pure PbZrO$_3$ (PZ) and PbTiO$_3$ (PT) materials this kind of relaxation has not been observed. Therefore the compositional disorder introduced by Ti and Zr is most essential, but introduction of La does not affect the principal mechanism of polarization; it merely changes their contribution to ε^*. Really, concerning Debye relaxors the following differences, with regard to the behaviour of PZT [47, 48] and PLZT 8/65/35 (figure 2, curve 1, interval II for PLZT) can be seen:

(1) ν_{IIm} for PZT is observed at 10^8–10^9 Hz [47, 48], and for PLZT in the 10^5–10^7 Hz interval [8, 9] (figure 2);

(2) The Debye mechanism is easily distinguished in PZT ceramics both around T_c (250–300 $^{\circ}$C) and at 20 $^{\circ}$C, while in PLZT ceramics, as mentioned above, it is seen only beyond $T_{m\varepsilon}$, i.e. mechanism II dominates in PZT, mechanism III being unnoticeable, whereas in PLZT both of them are comparable and coexistent.

At $\nu < 10^4$ Hz, $\varepsilon''(\nu)$ (figure 2, curve 1, frequency interval III) and $\varepsilon''(\varepsilon')$ are monotonic functions, i.e. the relaxation has a polydispersive nature. In terms of relaxation, according to the interpretation developed in studies of $\varepsilon^*(\nu)$ in PMN [50, 51], irreversible phase boundary motion is responsible for such a dispersion.

Thus, two polarization mechanisms in PLZT are represented by curve 1 in figure 2.

However, to provide microscopic interpretation, additional information obtained from dopant-induced transformations of the $\varepsilon^*(\nu, T)$ curve and from data of other structure-sensitive techniques is essential.

3.1.2. Dopant-induced changes. Essential changes are observed in $\varepsilon^*(\nu, E, T)$ [42–44] upon doping (figure 2, curves 2 and 3).

(1) $T_{m\varepsilon}$ shifts to a higher temperature.

(2) Relaxor properties become less pronounced in the interval 10^4–10^7 Hz as evidenced by the behaviour of $T_{m\varepsilon}(\nu)$; the quantitative changes are different in the sequence Mn > Co $\gtrsim$ Fe [42].

(3) The dispersion strength at $\nu < 10^4$ Hz is considerably enhanced and, in the case of Fe and Co, there is an $\varepsilon''(\nu)$ maximum in this interval (figure 2, curve 2, ν_{IIIm}), i.e. non-monotonic $\varepsilon''(\nu)$ and $\varepsilon''(\varepsilon')$ curves are observed which may be regarded as evidence of reversible elastic movement of phase boundaries (domain walls) (according to the interpretation developed in studies of similar behaviour of $\varepsilon^*(\nu)$ in PMN [50, 51]).

(4) The dispersion strength in the $\nu > 10^4$ Hz interval is considerably reduced (Mn > Fe, Co).

(5) The effects of electric field memory and temperature memory become weak (Fe and Co) or disappear completely (Mn) [44].

The following comments summarize the changes in $\varepsilon^*(\nu, T)$.

(1) The possible pre-critical or soft-mode behaviour of the lattice is changed as suggested by the $T_{m\varepsilon}$ shift [42] and the change in $\varepsilon''(\nu)$, $\varepsilon_l'(T)$ and $\varepsilon_h'(T)$ (unpublished results).

(2) The contribution of Debye-like relaxors (figure 2, curves 2 and 3; mechanism in the frequency range II) is reduced, but the contribution of slower large-scale relaxors has grown (figure 2; mechanisms in frequency range) at the same time. One may think of some reasons (possibly the change in the nature of the critical lattice mode mentioned) stimulating condensation of the individual relaxors in ensembles (clusters, correlated fluctuations, etc) and/or the disappearance of some individual relaxors.

3.2. Raman scattering

The Raman spectra of relaxor PLZT ceramics have been known for a long time [29]; however, little attention has been paid to relaxor properties [32]. Two particular problems related to different intervals of the spectrum may be distinguished for analysis: (a) firstly a broad central peak up to 100 cm^{-1} and (b) three broad bands beyond 100 cm^{-1} without an essential structure (figure 3, I, II and III).

3.2.1. 'Glass-like' and 'forbidden' bands of Raman spectra. Raman bands of the cubic structures (as detected by XRD [7, 9]) of relaxor PLZT compositions are 'forbidden' [52]. Broad bands are characteristic of disordered, i.e. glass or amorphous, structures [52]; for this reason these bands are referred to as 'glass like' [54, 55, 59, 65]. In this case RS represents a weighted average of the density of phonon states in the Brillouin zone [32, 52] and is caused by short-range translational disordering [28, 52] (contribution of the second-order processes in RS of PLZT seems to be small [32]; however, it may comprise a certain part of the observed spectrum at high temperatures [31]). The compositional disorder is assumed to be one of the primary sources of positional (structural) disordering, e.g. in PMN (its Raman spectrum is similar to PLZT) the 'glass-like' bands around 100–300 cm^{-1} are induced by
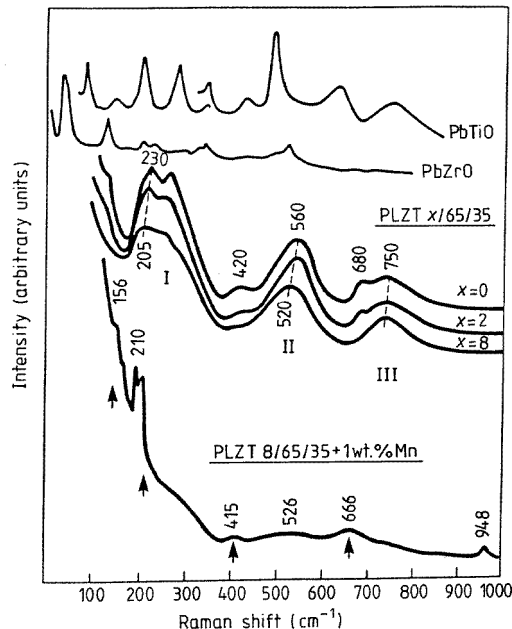
Figure 3. Room-temperature Raman spectra. PT and PZ spectra are from [57, 58] and [60, 61], respectively: I, II, III, 'glass-like' 'forbidden' bands. The arrows indicate bands induced on doping.

deviations of the local O–B–O bond angles from $90°$ $(180°)$, while those at 400–600 cm^{-1} are induced by local B–O bond radial stretch [53]. FE ordering caused by lowering the temperature or by modifying the structure [53] is indicated by the increase in intensity of some narrower bands. Static disorder prevails in the RS of glasses and amorphous structures [52]. However, in the case of relaxor and 'crossover' materials (i.e. of the BT type) the dynamic relaxing part of such disorder is important. The dynamic nature of the disorder is well disclosed in the BT structure which is compositionally ordered; however, similar bands are observed both at $T > T_c$ in the cubic phase and at $T < T_c$ in the tetragonal and orthorhombic phases [28], the 'glass-like' Raman bands here being a feature of the temperature interval of 'crossover' behaviour [25–29].

'Forbidden' 'glass-like' bands (I and II) are not observed in pure PT [57, 58] nor PZ [60, 61] (band III, which, due to its broadness, can be regarded as a 'glass-like' band, is observed in PT spectra; however, its origin is debatable and we shall not consider it here). They appear in PZT structures at certain PT (or PZ) concentrations and are very pronounced near the morphotropic phase boundary ([Zr]/[Ti] = 50/50) [62]. The 'glass-like' pattern of RS is additionally enhanced as La ions are introduced and the composition acquires cubic symmetry (XRD) and a very pronounced relaxor behaviour (figure 3; compare $x = 0$ and 2 at.% with $x = 8$ at.% for PLZT $x/65/35$) when the bands characteristic of PZ and/or PT structures have disappeared (except for III, as mentioned above).

The general 'glass-like' patterns of the RS of both the relaxor (PLZT) and the 'crossover' (BT) materials are similar. Nevertheless there are two essential points to be noted regarding the possible different kinds of disorder, and their different contributions to RS, in BT and PLZT. In the case of BT, the disorder is

(a) exclusively dynamic and

(b) relaxing Ti off-site ions are the only source.

In PLZT relaxor material the disorder is obviously 'stronger' and not only dynamic. The following sources of disorder can be distinguished in PLZT (not only Ti ions are relaxing):

(a) competing lattice distortion mechanisms due to PZ (orthorhombic phase) and PT (tetragonal phase) structures;

(b) compositional disordering and defectiveness of A sublattice caused by La^{3+} ions;

(c) disorder of the subsystem of non-bonding $6s^2$ electrons of Pb^{2+} ions [56].

Dynamic disorder of Ti off-site ions in BT is step by step reduced and 'frozen' correspondingly to long-range FE order transferring to the low-temperature tetrahedral and orthorhombic phases and disappearing completely in the rhombohedral phase. In the structure of PLZT its dynamic fraction of the disorder is reduced (frozen) more gradually, extending over a wide interval as the temperature is decreased [11]. In addition, that reduction in dynamic disorder is due to two processes: to 'freezing' of the disorder itself and to the emergence of some FE structure regions (the latter is suggested by the appearance of narrower bands in the spectrum at liquid-nitrogen temperature [29]). At $T > 20\,^{\circ}C$ there are no indications of structural ordering in RS above 100 cm^{-1} for PLZT 8/65/35, and only the irreversible phase boundary motion mechanism (figure 2, curve 1, region III) and the central peak in RS provide evidence of fluctuations in correlated ion displacements.

3.2.2. The central peak. The central peak together with the appearance of the soft-mode band provide information about the proximity of the spontaneously polarized state [25, 63, 64].

In relaxor materials a very pronounced component of quasielastic scattering, the central peak, its formation and growth (and subsequent disappearance as the material undergoes a transition to the state of polar glass [31]) indicate the presence of critical FE fluctuations. They can be characterized by the lifetime and correlation radius [66]. In real space, critical FE fluctuations might be imagined as coordinated shifts of one or more particular types of ion, possibly like a network of superpositioned chains which may stretch out over the crystal (grain) along a certain direction over some interval of time. There are strong reasons to support the fact that the central peak and glass-like bands (I and II) are essentially related to relaxing structures. If the relaxing element is more localized (regarding a unit cell or a few unit cells), it contributes to the 'glass-like' bands; if it is more extended and correlated, it shows up in the central peak. As the temperature is decreased and some correlated regions freeze, new narrower bands, reflecting an onset of FE ordered regions, may appear [29].

3.2.3. Dopant-induced change. The most essential effects observed in RS on doping (with Mn, Fe or Co) the PLZT 8/65/35 ceramics are (figure 3) [30]

(1) an increase in the central peak intensity,

(2) a decrease in the glass-like band intensity and

(3) the appearance of new bands at 156, 210, 415, 650–680 and 950 cm^{-1}.

The magnitude of these effects follows the sequence Mn $\rightarrow$ Fe $\rightarrow$ Co. Concerning the new dopant-induced bands it should be noted that, except for the approximately 950 cm^{-1} band, they are located firstly where the bands of PT, PZ and PLZT 0/65/35 are situated (figure 2) and secondly, in polarized (at 15 kV cm^{-1}) PLZT 8/65/35 samples where the 420 and 650–660 cm^{-1} bands (unpublished results) are likely to appear. Thus the dopant-induced changes in RS suggest that some structural ordering has occurred in the lattice.

3.3. EPR studies of PLZT 8/65/35 ceramics (spectra of Mn, Fe, Co and Cu)

The results of EPR studies on PLZT 8/65/35 (and PMN) ceramics have been reported elsewhere [67]. Hereafter we mainly concentrate on the following:

(a) conclusions drawn from EPR spectra of d^5 configurations (Mn^{2+}, Fe^{3+} and Co^{4+}) at negligible dopant concentrations (0.01 wt.%), causing essentially no change in either the structure or the properties, the d^5 ions serving as EPR probes of the original PLZT relaxor structure (i.e. non-modified structure);

(b) the Jahn–Teller (J–T) effect, i.e. the presence of Mn^{3+}, Fe^{4+}, Co^{5+} (d^4) and Cu^{2+} (d^9) ions which proved to be the primary reason for changes in structure and properties, the modifications being caused by dopants at sufficiently high concentrations (exceeding 0.1 wt.%);

(c) the change in d^5 ion spectra on modifying the PLZT structure, i.e. at sufficiently high d^4 ion concentrations and a small d^5 concentration, when d^5 ions serve as EPR probes of modified structure, and d^4 as modifiers.

3.3.1. Spectra of d^5 configuration ions; $g_{ef} \simeq 4.3$ absorption; probes of non-modified PLZT 8/65/35 structure ($[Me_{tot}] < 0.1$ wt.%). A characteristic feature of the spectrum is the dominating absorption at $g_{ef} \simeq 4.3$. The X-band spectrum of Fe (0.01 wt.%) at 20 °C is shown in figure 1(a) as an example. Less pronounced absorption in the EPR spectra of Mn, Fe and Co of unmodified (less than 0.1 wt.% Me_{tot}) PLZT is also observable at $g_{ef} \simeq 2.0$. However, here, regarding the unmodified structure, we concentrate on the $g_{ef} \simeq 4.3$ absorption, since just the latter is related to relaxor behaviour (see section 3.5.1).

A number of arguments such as

(a) the $g_{ef} \simeq 4.3$ absorption itself together with other features of spectra [46, 67],
(b) the $g_{ef} \simeq 4.3$ absorption (Mn and Fe) reported for polycrystals [68, 69] and
(c) the fact that this absorption is, as a rule, observed in Mn, Fe-doped disordered media [70–72]

suggest that the d^5 configurations (Fe^{3+}, Mn^{2+} and Co^{4+}) in a strong crystal field of fully rhombic symmetry are responsible for this absorption [68–73, 78–80]. In terms of the spin-Hamiltonian parameters D and E (representing the axial and rhombic deformation, respectively) this means, correspondingly that

(1) $|D|, |E| \gg h\nu$ (practically $|D|, |E| > 0.6h\nu$ is sufficient [72], where ν is the microwave frequency),
(2) $D/E = 3$ [68–72] and
(3) a broad distribution of D and E ($\Delta D \neq 0$ and $\Delta E \neq 0$) around and including $D/E = 3$.

Thus, certain conclusions can be made with regard to the geometry of d^5 ion environment, i.e. to deformations of MeO_6^{2-} octahedra in relaxor-type PLZT 8/65/35.

(i) There are very strong (large magnitude) deviations of the O–B distances from ideal cubic symmetry positions, i.e. of the order of more than 0.1 Å, or deviations of the O–B–O angles by several degrees from 90° (180°) [70, 72] but, because the d^5 ions tend to occupy the centres of oxygen octahedra (the in-site but not the off-site positions) and in particularly, if they are acceptors such as Me^{2+} and Me^{3+}, the EPR spectra of Mn^{2+} and Fe^{3+} basically reflect strong deviations of O_6^{2-} ions from cubic sites (Co^{4+} might also occupy the off-site positions) [27].

(ii) As the $g_{ef} \simeq 2.0$ absorption ($|D|$, $|E| < 0.6h\nu$) is weak, the concentration of 'cubic' centres, i.e. weakly deformed O_6^{2-} [70], is small.

Figure 1(e) provides some illustration of the evolution of Fe^{3+} EPR spectra in the composition series PT $\rightarrow$ PZT $\rightarrow$ PLZT1/65/35 $\rightarrow$ PLZT 8/65/35. Similar to RS where the completely 'glass-like' unstructured bands appear at a certain concentration of La (figure 3), the shapes of the $g_{ef} \simeq 4.3$ absorption in PLZT x/65/35 become completely similar to those observed in glasses and disordered structures [71] only at $x \geqslant 8$ (figure 1(e)). Thus, the compositional and structural reasons for the $g_{ef} \simeq 4.3$ absorption in relaxor PLZT appear to be similar to the BO_6^{2-} deformations mentioned above in the discussion of the 'glass-like' and 'forbidden' bands in RS (structural disorder).

Phenomena observed in PLZT material as described above (Debye-like relaxation from $\varepsilon^*(\nu, T)$; amorphous 'glass-like' Raman bands and $g_{ef} \simeq 4.3$ absorption in EPR spectra) are due to the La/Ti/Zr proportions and the particular compositional disordering related to these. The compositional disordering is followed by certain structural disordering which is probably not detected by XRD.

3.3.2. Jahn–Teller effect; the reason for modification (at $[Me_{tot}] \geqslant 0.1$ wt.%). The microscopic origins of the fundamental (i.e. bulk) effects [42, 45] in the structure and properties of PLZT 8/65/35 caused by the admixture of $[Me_{tot}] \geqslant 0.1$ wt.%, and observed by XRD [42, 45], RS [30] and other methods had not been revealed until EPR results were employed. The qualitative and quantitative changes observed in the d^5 and Cu^{2+} spectra with change in the dopant concentration [46, 67] (figures 1(a) and (1(c)) together with oxidation–reduction experiments on the modified samples (an example of the Fe case is demonstrated in figure 1(d)) compared with other data (the shift in T_{me} (figures 1(a)–1(d)) have proved the J–T effect, i.e. the presence of dopants as d^4 configuration ions (Mn^{3+}, Fe^{4+} and Co^{5+}) and d^9 (configuration ions (Cu^{2+}) which are mainly responsible for the observed dopant-induced modifications.

In fact, in the case of Cu the spectrum (figure 1(c)) is due to Cu^{2+} (d^9), i.e. J–T ions. The area S under the absorption curves is proportional to the concentration $[Me_{ld^9}]$ of Cu^{2+} ions (S_{d^9}) in the lattice and follows its change. From $\Delta T_{m\varepsilon}([Me]_{tot})$ it is seen that $S_{d^9} \sim \Delta T_{m\varepsilon}$, i.e. J–T effect is responsible for the shift in $T_{m\varepsilon}$ to a higher temperature. The possible change in spontaneous polarization and increases in T_c (the Curie point), caused by the J–T effect has been discussed earlier [74–76] and is not unexpected. (However, if non J–T configurations, i.e. Cu^+, Cu^{3+} and Cu^{4+} prevailed [74] or the oxygen vacancies V_O supported local electroneutrality, a decrease in T_c would be possible.)

Obviously, in PLZT+Mn, Fe, Co samples some of the J–T ions are d^4 ions (Mn^{3+}, Fe^{4+} and Co^{5+}) and $\Delta T_{m\varepsilon} \sim [Me_{ld^4}]$ while d^5 configurations (Mn^{2+}, Fe^{3+} and Co^{4+}) are the EPR probes, the area under absorption curves S_{d^5} being proportional to the Me_{ld^5} concentration: $S_{d^5} \sim [Me_{ld^5}]$.

In the case when conventional two-stage hot pressing is used to manufacture the PLZT+Mn, Fe, Co samples, $[Me_{ld^5}] \ll [Me_{ld^4}]$ in the modified material ($[Me_{tot}] > 0.1$ wt.%) as observed earlier [67]. For that reason the d^5 ions should be regarded as probes of the modified structure, provided that the probes are uniformly distributed in the sample (figures 1(a) and 1(b)). The features of the modified structure and the changes in d^5 spectra occurring with increase in the Me concentration will be discussed later. Next we pay attention exclusively to the J–T effect.

The coexistence of d^4 and d^5 ions ($d^4 + e \rightarrow d^5$) predetermines the possible change in the $[Me_{ld^4}]/[Me_{ld^5}]$ ratio, i.e. the modifying efficiency by changing the oxidation–

reduction conditions; the latter is demonstrated in figure 1(d). A PLZT 8/65/35+1 wt.% Fe ($T_{me} = 145\,°C$) sample has been selected for reference, the corresponding d^5 absorption reference curves being given in figures 1(a) and (1(b). As the reducing efficiency is enhanced (20 h $\rightarrow$ 3 h $\rightarrow$ 0.5 h; see sample technology and [67]) and the $Fe^{4+} + e \rightarrow Fe^{3+}$ reaction enforced, $S_{d^5} \sim [Me_{ld^5}]$ increases, while the $[Me_{ld^4}]/[Me_{ld^5}]$ ratio and ΔT_{me} are decreased ($55\,°C \rightarrow 45\,°C \rightarrow -5\,°C$). In strongly reduced samples (e.g. Figure 1(d), where the corresponding curve is denoted by 0.05 h, $T_{me} = 85\,°C$) the concentration of d^5 is fairly high and maybe as large as $[Me_{ld^5} \gg [Me_{ld^4}]$, and the d^5 ions cannot serve as neutral probes having a negligible influence on the structure.

3.3.3. Spectra of d^5 configurations; probes in a modified PLZT 8/65/35 structure ($[Me] \geqslant 0.1$ wt.%; $g_{ef} \simeq 2.0$ absorption). A broad EPR component at $g_{ef} \simeq 2.0$ appears (or is enhanced if present) on increase in the dopant concentration (figure 1(a), Fe), i.e. with increase in the J–T ion (d^4 modifier) concentration. The intensity of this component increases compared with the intensity of the $g_{ef} \simeq 4.3$ component, i.e. the intensity ratio of the $g_{ef} \simeq 2.0$ component to the $g_{ef} \simeq 4.3$ component increases. However, the 'glass-like' nature of the spectrum is still maintained, at least partially. In fact, the $g_{ef} \simeq 4.3$ absorption is still present. It also has to be remembered that the 'glass-like' nature of RS does not disappear completely in modified PLZT (figure 3).

The latter condition means that the neighbourhood of these centres, i.e. the O_6^{2-} octahedra, has a considerably smaller deformation than the centres responsible for the $g_{ef} \simeq 4.3$ absorption (see above). Also, it is essential to note that the hyperfine structure (HFS) of the $g_{ef} \simeq 2.0$ absorption is almost not resolvable in the X band, but it is possible to resolve it in the Q band (the HFS constant $A = 105 \pm 5$ G for Mn [46]. This is evidence of some distribution in the parameters D and E, i.e. ΔD, $\Delta E \neq 0$, and $|D \pm \Delta D|$, $|E \pm \Delta E| < 0.6h\nu$.

On the other hand, we know that the appearance of new bands in RS [30] (figure 2) and signs of monoclinic distortion in XRD [42] (see text below) confirm the presence of some fraction of FE phase (regions less than 500 Å) in modified PLZT. From the EPR spectra of the d^5 ion probes in FE materials [81, 82] it may be concluded that, first, $h\nu > |E|$, $|D| > 0$ and ΔD, $\Delta E \simeq 0$ and, second, the majority of the components of the d^5 resonances (particularly those for which E and D are far from zero) are 'extremely anisotropic', i.e. in the case of polycrystals these resonances would smear out. Thus we think that some fraction of the FE phase may provide a certain but not an essential contribution to the $g_{ef} \simeq 2.0$ absorption in our case. The fraction of transitional regions between FE and the 'old', 'glass-like' structure is obviously dominating.

Thus, the EPR results allow us to say that the new modified structure is a heterogeneous mixture of three different structures. In terms of spin-Hamiltonian parameters which, first of all, are characteristics of the O_6^{2-} deformations, the three structures (phases) are distinguished as follows:

(1) $h\nu > |D|$, $|E| > 0$; ΔD, $\Delta E = 0$ (the FE phase, the spectrum is smeared);
(2) $h\nu > |D \pm \Delta D|$, $|E \pm \Delta E|$; ΔD, $\Delta E \neq 0$; $g_{ef} \simeq 2.0$ (transitional phase);
(3) $|D \pm \Delta D|$, $|E \pm \Delta E| > 0.6h\nu$; $g_{ef} \simeq 4.3$ ('glass-like' phase).

Also, it is worth noting that in the case of Co^{4+} the Q-band spectrum probably has a double hyperfine structure (only if it is not related to forbidden hyperfine transitions, which is not clear so far). Different from Mn^{2+} reflecting the in-site positions, Co^{4+} tends to reflect the off-site positions (B ion sites) as well. In this case the double HFS of Co^{4+} ion absorption indicates the possible existence of two different positions of B ions.

3.3.4. Essential features of admixture (Mn, Fe, Co) implantation in the PLZT lattice. With respect to the PLZT+Mn, Fe, Co samples obtained by the conventional two-stage hot-pressing techniques the following can be concluded.

(1) Me ions implanted in the lattice (Me_l) are characterized by a distribution of valencies, the maximum corresponding to the valency of the d^4 configuration. This means that in the series Mn $\rightarrow$ Fe $\rightarrow$ Co the maximum complies with a fixed configuration d^4, i.e. the lattice has forced (imposed and freezed) the configuration (possibly it is connected with the soft mode), the valency being adapted, so that $[Me_{ld^4}] \gg [Me_{ld^5}]$. Thus there are modifying ions, Me_{ld^4}, and EPR probes, Me_{ld^5}, in the lattice. Another situation may appear in samples produced (or treated) in a strongly reducing medium; see, for example, the case of PLZT+1 wt.% Fe (figure 1(d)) where external reducing conditions change the valency.

(2) The local electroneutrality is obviously predominantly supported by electron processes, e.g. Mn^{3+}–Pb^{3+}, Mn^{3+}–La^{3+} or Co^{5+}–Ti^{3+} etc (V_O, which compensates Fe^{3+}, is obviously present in the sample illustrated in figure 1(d) by the 0.5 h curve as suggested by firstly the $g_{ef} \simeq 6.0$ component in the spectrum, i.e. the axial pair Fe^{3+}–V_O [69], and secondly the $g_{ef} \simeq 2.0$ component, since the latter is present at such degrees of reduction in PLZT 8/65/35 samples without any Fe admixture, i.e. the $g_{ef} \simeq 2.0$ absorption here is not related to structural ordering or the J–T effect as discussed previously, but to the oxygen vacancy V_O in the role of F centre [77, 83].)

3.4. X-ray diffraction studies

3.4.1. Undoped PLZT. At first sight it seems that there is a contradiction between the $g_{ef} \simeq 4.3$ absorption discussed in section 3.3.1 and the well known XRD data suggesting a cubic perovskite structure of PLZT 8/65/35 down to liquid-nitrogen temperature [2, 19]. However, the results obtained by high-resolution XRD techniques [13] confirm and supplement conclusions drawn from Raman and EPR data concerning the microstructure. It has been reported [13] that

(1) fluctuations of lattice deformation (rhombohedral distortions) and polarization at the unit-cell level appear at $T < 640\,^\circ$C and
(2) the root mean square displacements of BO_6^{2-} ions increase markedly as the temperature is lowered (it is logical to call this structure a 'pseudo-cubic' [13]).

3.4.2. Dopant effects. Three effects are observed in the XRD pattern upon doping (Mn, Fe and Co) [42, 45]:

(1) a shift in the diffraction maxima towards large angles, the lattice parameter $\bar{a} = \sqrt[3]{V_{uc}}$ (V_{uc} is the unit-cell volume) being reduced;
(2) an asymmetric broadening of diffraction maxima at medium and large angles and splitting on increase in the dopant concentration; analysis of the splitting of 222 and 220 reflections of Co Kα radiation suggests a monoclinic distortion (in the case of Fe and Co) which indicates intrinsic electric-field-induced phenomena [2] of the original 'pseudo-cubic' cell;
(3) on increase in the ratio of integrated intensities of diffraction maxima with different numbers of even indices, e.g. I_{210}/I_{211}.

The effects increase in the sequence Mn $\rightarrow$ Co $\rightarrow$ Fe(Mn > Co $\gtrsim$ Fe) [42, 45].

3.5. Correlation between polarization mechanisms (weak fields) and the structure

In this section the dielectric permittivity dispersion (polarization mechanisms) and corresponding structure conditions (structural elements; subsystems; size and time indications) are discussed.

3.5.1. Correlations in the sequence PT, $PZ \to PZT \to PLZT$; behaviour of undoped PLZT 8/65/35. The three characteristic phenomena observed with correlations in the sequence PT, PZ → PZT → PLZT as described above, namely

(a) Debye-like (i.e. nearly monodispersive) ε'' relaxation in the frequency interval 10^4 Hz $< \nu < 10^9$ Hz ($T > 20\,°$C);
(b) 'glass-like' and 'forbidden' bands in RS ($20\,°$C) and
(c) EPR at $g_{ef} \simeq 4.3$ ($20\,°$C),

first of all appear simultaneously on formation of PZT from PT and PZ and become completely pronounced when a sufficiently high concentration of La ions is reached, providing relaxor-type PLZT. This indicates the short-range disorder of the BO_6^2-subsystem (discussed with regard to EPR and RS results) as a necessary condition of Debye-like relaxation.

Obviously, only some of all the BO_6^{2-} octahedra participate in this polarization process. In the first approximation these octahedra have deformations, the type and direction of which are favourably oriented with respect to the applied field. Presumably such a single octahedron is imagined as the elementary relaxing particle or its 'seed'. It seems essential that the Ti ion has a higher freedom (its ion radius is smaller than that of Zr), i.e. mobility (similar to Ti off-site in BT [26, 27]), inside a distorted octahedron.

As the temperature decreases, firstly the individual relaxing dipoles join into clusters by a nearest-neighbour or 'intracluster interaction' [22, 23] which is manifested by the appearance of polydispersive relaxation in the 10^4–10^8 Hz interval, and secondly an 'intercluster' interaction [22, 23] appears, contributing to dispersion at $\nu < 10^4$ Hz (monotonic $\varepsilon''(\nu)$ and $\varepsilon''(\varepsilon')$ (figure 2, curve 1, region III)) and to an increase in the central peak component in RS (FE critical fluctuations). As the temperature continues to decrease both the dispersion regions strongly superimpose; some of the relaxors freeze, and the 'polar glass' structure is formed. However, it should be noted once more that the 'polar glass' structure in PLZT 8/65/35 is not revealed by XRD and rather conditionally by RS and EPR.

Summarizing, relaxor behaviour of the incipient undoped PLZT/8/65/35 in the Curie range, as follows from the previous discussion, is characterized by

(1) Debye-like (i.e. nearly monodispersive) relaxation in the 10^4–10^8 Hz interval and a moderately pronounced monotonic $\varepsilon''(\nu)$ and $\varepsilon''(\varepsilon')$ curves (polydispersive) in the 10^{-1}–10^4 Hz interval at $T > T_{m\varepsilon}$ (figure 2, curve 1) (consequently, there are two separate and different polarization mechanisms contributing to the dielectric permittivity: elementary relaxing particle switching and non-reversible phase boundary motion),
(2) $T_{m\varepsilon} \simeq 90\,°$C ($10^4$ Hz) and a strongly pronounced dependence of $T_{m\varepsilon}$ on the frequency in the 10^3–10^7 Hz interval [42] and
(3) the presence of the effects of thermal and electric field memory [44].

At the same time the structure in the thermally depolarized state at $20\,°$C corresponding to this behaviour is defined by

(1) a cubic (pseudo-cubic) XRD pattern (with $\bar{a} = 4.070$ Å and $I_{210}/I_{211} = 0.15$ [42]),

(2) a rather broad central peak below 100 cm^{-1} and 'glass-like' 'forbidden' bands above 100 cm^{-1} in RS [30] (figure 3),

(3) dominating absorption at $g_{ef} \simeq 4.3$ in EPR spectra (figure 3) (Fe ions as probes),

(4) lack of domain structure,

(5) Poisson's coefficient $\sigma_P = 0.29$ [42] and

(6) brittle cleavage and plastic deformation in the transgranular fracture pattern [45].

3.5.2. Dopant effects in PLZT 8/65/35; appearance of 'non-relaxor' behaviour. If the structure of the modified PLZT 8/65/35 composition and its behaviour are compared with the incipient relaxor structure and behaviour as defined above, one has to conclude that the modified composition does not fit the idea of a relaxor. On the other hand, the new structure in the cases of Mn, Fe and Co does not fit a proper definition of the FE structure.

Really, the long-range order of the spontaneously polarized static FE state is not attained by the dopant admixture, but the trend is clearly observed and evidenced by

(a) the shift of $T_{m\varepsilon}$ (Curie region) to a higher temperature,

(b) the appearance of new Raman bands existing in RS of PT and/or PZ (dominates on doping with Fe or Co) and increases in the central peak (dominates on doping with Mn) as possible evidence of FE regions and

(c) signs of monoclinic distortion in the XRD pattern (dominates on doping with Fe, Co), etc.

In the ε behaviour of incipient PLZT 8/65/35 at $T_{m\varepsilon} + 10\,^{\circ}\mathrm{C}$ and $\nu < 10^4$ Hz the irreversible phase boundary motion dominates over reversible elastic phase boundary motion (or the latter cannot be distinguished on the $\varepsilon''(\nu)$ curve or this mechanism is not present) (figure 2, curve 1). At 20 °C a broad superposition of the different mechanisms (elementary relaxing particles, clusters and irreversible phase boundary motion) is observed. Modification, as suggested by the $\varepsilon''(\nu)$ behaviour (figure 2, curves 2 and 3), seems to have enhanced the low-frequency (region III) mechanisms (irreversible phase boundary motion in the case of Mn and elastic reversible phase boundary motion in the case of Fe and Co) and suppressed Debye-like relaxation (region II). These characteristic and notable modifications of $\varepsilon(\nu, T, E)$ combine with characteristic rearrangements of the structure.

The most essential relations are firstly the irreversible phase boundary motion (from $\varepsilon''(\nu)$) $\leftrightarrow$ FE critical fluctuations (from the central peak in RS) and secondly elastic reversible phase boundary motion $\leftrightarrow$ the presence of FE microregions (domains) (from XRD and TEM [45]).

Thus, the previous rather abstractly defined polarization mechanisms [5, 50, 51] in principle may be related to particular compositional and structural elements or subsystems.

It is essential that the magnitude of most of the dopant-induced effects follows either the sequence Mn > Fe $\gtrsim$ Co or the sequence Co $\geqslant$ Fe > Mn. The following interpretation has been proposed elsewhere:

(1) In the case of Mn, effects which might be called cooperative dynamic effects of admixture J–T ions dominate.

(2) In contrast in the case of Fe and Co, the effects are induced by the static electric fields of the J–T static dipoles (similar to monoclinic distortion [42]).

The quantitative difference in the sequence Mn → Fe → Co might be explained by

(1) the difference in the ion radii of the d^4 configuration (here Mn^{3+} > Fe^{4+}) (the J–T ion can be represented as a static dipole, and, the smaller the ion, the stronger is the dopole) and

(2) the difference in the effects caused by local electroneutrality conditions of the d^4 ion configuration (Mn^{3+}, Co^{5+} and Fe^{4+}), e.g. Mn^{3+}–Pb^{3+} or Mn^{3+}–La^{3+} or Co^{5+}–Ti^{3+}, while in the case of Fe^{4+} no adjustment of the surroundings is needed.

It should be noted that by understanding the microscopic reasons for the different dopant effects observed with Mn, Fe and Co in PLZT ceramics one may obviously find the answer to the question of why the admixture of Mn in PZT ceramics acts as a 'stabilizer' of the material properties, while Fe acts as a 'hardener' [20, 84, 85].

4. Conclusions

(1) The structural conditions ($20\,^\circ$C) for the existence of proposed elementary relaxing particles (Debye-like relaxors, in terms of the $\varepsilon(\nu)$ behaviour) are revealed in the PLZT composition.

(2) Three polarization mechanisms related to specific structural conditions ($20\,^\circ$C) are shown to exist in modified PLZT 8/65/35 ceramics in the Curie region. This means that $\varepsilon(T, \nu, E)$ behaviour of PLZT compositions is predictable from the structure peculiarities at $20\,^\circ$C (determined by a complex set of techniques, e.g. EPR, XRD, RS and others).

(3) The studies of modified PLZT 8/65/35 compositions demonstrate that

(a) EPR spectra of Mn^{2+}, Fe^{3+} and Co^{4+} ions can be used as probes to detect relaxor or disordered perovskite structure,

(b) the most essential dopant-induced effects on the structure and behaviour are due to J–T configurations of the admixture ions and

(c) two different manifestations of the J–T effects in PLZT are similar to those of well known 'hardeners' and 'stabilizers' in modifying PZT ceramics by Mn and Fe.

Acknowledgments

References

[1] Lines M E and Glass A M 1977 *Principles and Application of Ferroelectrics and Related Materials* (Oxford: Clarendon)
[2] Isupov V A 1992 *Ferroelectrics* **131** 41
[3] Smolensky G A 1970 *J. Phys. Soc. Japan Suppl.* **28** 26
[4] Bokov A A 1992 *Ferroelectrics* **131** 49
[5] Cross L E 1987 *Ferroelectrics* **76** 241
[6] Viehland D, Jang S J and Cross L E 1990 *J. Appl. Phys.* **68** 2916
[7] Viehland D, Wuttig M and Cross L E 1991 *Ferroelectrics* **120** 71
[8] Kersten O, Rost A and Schmidt G 1983 *Phys. Status Solidi* a **75** 495
[9] Schmitt H and Dorr A 1989 *Ferroelectrics* **93** 309
[10] Laiho R, Lushnikov S and Siny I 1992 *Ferroelectrics* **125** 493
[11] Yushin N K, Bazarova L F and Gulyanov G 1989 *Ferroelectrics* **90** 57
[12] Smolensky G 1984 *Ferroelectrics* **53** 129
[13] Darlington C N W 1989 *J. Phys. C: Solid State Phys.* **21** 3851
[14] Burns G and Dacol F H 1983 *Phys. Rev.* B **28** 2527
[15] Thomas N W 1990 *J. Phys. Chem. Solids* **51** 1419
[16] Reineke T and Ngai K 1976 *Solid State Commun.* **18** 1543
[17] Bokov A A and Rayevsky I P 1989 *Ferroelectrics* **90** 125

[18] Mathan N, Husson E, Gaucher P and Morell A 1990 *Mater. Res. Bull.* **25** 427
[19] Haertling G and Land C 1971 *J. Am. Ceram. Soc.* **54** 1
[20] Jaffe B, Cook W R and Jaffe H 1971 *Piezoelectric Ceramics* (London: Academic)
[21] Isupov V A 1989 *Ferroelectrics* **90** 113
[22] Jonscher A K 1983 *Dielectric Relaxation in Solids* (London: Chelsea Dielectric)
[23] Ngai K L and White C T 1979 *Phys. Rev.* B **20** 2475
[24] Dissado L A and Hill R M 1980 *Phil. Mag.* B **41** 625
[25] Gervais F 1984 *Ferroelectrics* **53** 91
[26] Itoh K, Zheng L Z, Nakamura E and Mishima N 1985 *Ferroelectrics* **63** 29
[27] Müller K A 1986 *Helv. Phys. Acta* **59** 874
[28] Jannot B and Gnininvi L 1981 *Ferroelectrics* **37** 669
[29] Lurio A and Burns G 1974 *J. Appl. Phys.* **45** 1986
[30] Dimza V, Paulins P, Zhang M S, Chen Q and Lin Z 1992 *Ferroelectrics* **131** 239
[31] Prokhorova S D and Lushnikov S G 1989 *Ferroelectrics* **90** 187
[32] Burns G and Scott B A 1973 *Solid State Commun.* **13** 423
[33] Kersten O 1986 *KTB Wiss. Beitr. (Halle/Wittenberg: Martin-Luther-Univers)* **66** 118
[34] Khatib D, Migoni R, Kugel G E and Godefroy L 1989 *J. Phys.: Condens. Matter* **1** 8811
[35] Lyons K B, Fleury P A and Rytz D 1986 *Phys. Rev. Lett.* **57** 2207
[36] Hochli U T and Maglione M 1989 *J. Phys.: Condens. Matter* **1** 2241
     Sommer D, Kleemann W and Rytz D 1990 *Ferroelectrics* **106** 137
[37] Vugmeister B E and Glinchuk M D 1990 *Rev. Mod. Phys.* **62** 993
[38] Banfi G P, Calvi P, Ginlotto E and Samoggia G 1990 *Ferroelectrics* **106** 143
[39] Klein R S, Kugel G E, Fontana M D and Höchli U T 1992 *Ferroelectrics* **125** 325
[40] Bonziane E, Fontana M D and Kugel G E 1992 *Ferroelectrics* **125** 331
[41] Leschenko M A, Poplavko Yu M and Bovtun V P 1992 *Ferroelectrics* **131** 213
[42] Dimza V I, Sprogis A A, Kapenieks A E, Shebanov L A, Plaude A V, Stumpe R and Books M 1989
     Ferroelectrics **90** 45
[43] Burkhanov A I, Shilnikov A V and Dimza V I 1995 at press
[44] Burkhanov A I, Shilnikov A V and Dimza V I 1992 *Ferroelectrics* **131** 267
[45] Dimza V, Plaude A, Chengui L, Duan F, Hanmi L and Jingson Z 1992 *Ferroelectrics* **131** 249
     Plaude A 1992 *Ferroelectrics* **131** 247
[46] Dimza V, Jing T Z, Han S Y, Xu Y, Glinchuk M D, Bikov I P and Skorokhod V V 1992 *Phys. Status Solidi*
     a **132** K93
[47] Kersten O and Schmidt G 1986 *Ferroelectrics* **67** 191
[48] Kersten O, Hofman M and Schmidt G 1986 *Ferroelectrics* **6** 75
[49] Kersten O, Rost A and Schmidt G 1988 *Ferroelectrics* **81** 31
[50] Nadolinskaja E G, Krainik N N and Shilnikov A V 1988 *Sov. Phys.–Solid State* **30** 149 (in Russian)
[51] Shilnikov A V, Galijarova N M, Gorin S V, Vasiljev D G and Vologirova L X 1991 *Bull. Acad. Sci. USSR,*
     Capt. Phys. **55** 578
[52] Cardona M (ed) 1975 *Light Scattering in Solids* (Berlin: Springer)
[53] Husson E, Abello L and Morell A 1990 *Mater. Res. Bull.* **25** 539
[54] Harley R T, Page J B and Walker Ch T 1971 *Phys. Rev.* B **3** 1365
[55] Hilbert Ch, Stranch D, Miuanaga T and Luty F 1989 *J. Phys.: Condens. Matter* **1** 1381
[56] Alonso J A and Rasines I 1988 *J. Phys. Chem. Solids* **49** 385
[57] Tornberg N E and Perry C H 1970 *J. Chem. Phys.* **53** 2946
[58] Burns G and Scott B A 1970 *Phys. Lett.* **25** 168
[59] Takashige M, Nakamura T and Aikava I 1983 *Ferroelectr. Lett.* **44** 313
[60] Pasto A E and Condrate R A 1973 *J. Am. Ceram. Soc.* **56** 436
[61] Li S, Condrate R A, Jang S D and Spriggs R M 1989 *J. Mater. Sci.* **24** 3873
[62] Bäuerle D, Holzapfel W B, Pinzuk A and Jacoby J 1977 *Phys. Status Solidi* b **83** 99
[63] Bruce A D, Taylor W and Murray A F 1980 *J. Phys. C: Solid State Phys.* **13** 483
[64] Aksenov V L, Bobeth M and Plakida N M 1987 *Z. Phys.* B **69** 393
[65] Salje E and Bismayer U 1989 *J. Phys.: Condens. Matter* **1** 6967
[66] Vakhrushev S B, Kvyatkovsky B E, Naberezhnova A A, Okuneva N M and Toperverg B P 1989 *Ferroelectrics*
     90 173
[67] Dimza V I 1993 *Phys. Status Solidi* a **140** 543
[68] Dowsing R D and Gibson J F 1969 *J. Chem. Phys.* **50** 294
[69] Aasa R 1970 *J. Chem. Phys.* **52** 3919

[70] Kliava J 1986 *Phys. Status Solidi* b **134** 411
[71] Rao K J and Rao B G 1985 *Proc. Indian Acad. Sci. (Chem. Sci.)* **95** 169
[72] Brodbeck C M and Bukrey R R 1981 *Phys. Rev.* B **24** 2334
[73] Kutty T R N and Balachandran R 1985 *Mater. Chem. Phys.* **13** 467
[74] Kristofel N N 1981 *Fiz. Tverd. Tela* **23** 3267
[75] Venevtsev Yu, Dzhmuhadze D F, Fadeeva N V and Ivanov S A 1988 *Ferroelectrics* **79** 229
[76] Bersuker G I 1988 *Phys. Status Solidi* b **148** 243
[77] Wertheim G K, Hausman A and Sander W 1971 *The Electronic Structure of Point Defects* (Amsterdam: North-Holland)
[78] Hennings D and Pomplun H 1974 *J. Am. Ceram. Soc.* **57** 527
[79] Molak A and Vojcik K 1992 *Ferroelectrics* **125** 349
[80] Kutty T R N, Murugaraj P and Gajbhige N S 1985 *Mater. Res. Bull.* **20** 565
[81] Sakudo T 1963 *J. Phys. Soc. Japan* **18** 1626
[82] Possenriede E, Shirmer O F, Donnenberg H J and Hellerman B 1989 *J. Phys.: Condens. Matter* **1** 7267
[83] Wertz J E and Bolton J R 1972 *Electron Spin Resonance* (New York: McGraw-Hill)
[84] Wersing W 1976 *Ferroelectrics* **12** 143
[85] Eyraud L, Gonnard P and Claudel B 1990 *J. Am. Ceram. Soc.* **73** 1854